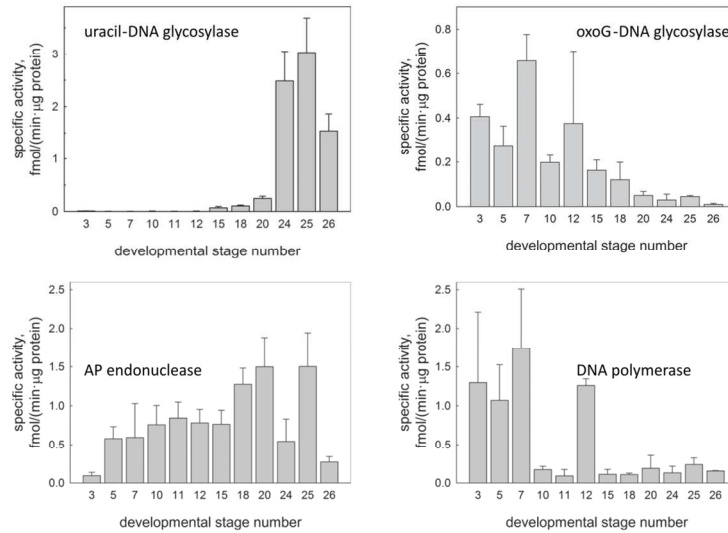




**Base excision DNA repair in the embryonic development of
the sea urchin, *Strongylocentrotus intermedius***

Journal:	<i>Molecular BioSystems</i>
Manuscript ID	MB-ART-12-2015-000906.R1
Article Type:	Paper
Date Submitted by the Author:	09-Apr-2016
Complete List of Authors:	Torgasheva, Natalya ; Institute of Biological Chemistry and Fundamental Medicine, Siberian Division of Russian Academy of Sciences Menzorova, Natalya ; G. B. Elyakov Pacific Institute of Bioorganic Chemistry, FEB RAS Sibirtsev, Yuri ; G. B. Elyakov Pacific Institute of Bioorganic Chemistry, FEB RAS Rasskazov, Valery ; G. B. Elyakov Pacific Institute of Bioorganic Chemistry, FEB RAS Zharkov, Dmitry ; Institute of Biological Chemistry and Fundamental Medicine, Siberian Division of Russian Academy of Sciences Nevinsky, Georgy; Institute of Biological Chemistry and Fundamental Medicine, Siberian Division of Russian Academy of Sciences

In actively proliferating cells, such as cells of the developing embryo, DNA repair is crucial for preventing accumulation of mutations and synchronizing cell division. We have characterized the profile of several key base excision repair activities in the developing embryos (2 blastomers to mid-pluteus) of the grey sea urchin, *Strongylocentrotus intermedius*.



Specific activity of uracil–DNA glycosylase , 8-oxoguanine–DNA glycosylase, AP endonuclease, and specific gap-filling DNA polymerase at 26 different stages of *S. intermedius* development.

130x102mm (300 × 300 DPI)

Base excision DNA repair in the embryonic development of the sea urchin, *Strongylocentrotus intermedius*

Natalya A. Torgasheva^{a,b}, Natalya I. Menzorova^c, Yurii T. Sibirtsev^c, Valery A. Rasskazov^c,
Dmitry O. Zharkov^{a,b*}, Georgy A. Nevinsky^{a,b*}

^a*Institute of Chemical Biology and Fundamental Medicine SB RAS, 8 Lavrentieva Ave., Novosibirsk 630090, Russia*

^b*Novosibirsk State University, 2 Pirogova St., Novosibirsk 630090, Russia*

^c*G. B. Elyakov Pacific Institute of Bioorganic Chemistry FEB RAS, 159 100 let Vladivostoku Ave., Vladivostok 690022, Russia*

In actively proliferating cells, such as cells of the developing embryo, DNA repair is crucial for preventing accumulation of mutations and synchronizing cell division. Sea urchin embryo growth was analyzed and extracts were prepared. The relative activity of DNA polymerase, apurinic/aprimidinic (AP) endonuclease, uracil–DNA glycosylase, 8-oxoguanine–DNA glycosylase, and other glycosylases were analyzed using specific oligonucleotide substrates of these enzymes; the reaction products were resolved by denaturing 20% polyacrylamide gel electrophoresis. We have characterized the profile of several key base excision repair activities in the developing embryos (2 blastomers to mid-pluteus) of the grey sea urchin, *Strongylocentrotus intermedius*. The uracil–DNA glycosylase specific activity sharply increased after blastula hatching, whereas the specific activity of 8-oxoguanine–DNA glycosylase steadily decreased over the course of the development. The AP-endonuclease activity gradually increased but dropped at the last sampled stage (mid-pluteus 2). The DNA polymerase activity was high at the first cleavage divisions and then quickly decreased, showing a transient peak at blastula hatching. It seems that the developing sea urchin embryo encounters different DNA-damaging factors early in development within the protective envelope and later as a free-floating larva, with hatching necessitating adaptation to the shift in genotoxic stress conditions. No correlation was observed between the dynamics of the enzyme activities and published gene expression data from developing congeneric species, *S. purpuratus*. The results suggest that base excision repair enzymes may be regulated in the sea urchin embryos at the level of covalent modification or protein stability.

Keywords: DNA damage, DNA repair, DNA glycosylases, AP endonucleases, DNA polymerases, embryonic development, sea urchin

Abbreviations: AP, apurinic/apyrimidinic; BER, base excision repair; DTT, dithiothreitol; EDTA, ethylenediaminetetraacetate; MYP, major yolk protein; oxoG, 8-oxoguanine; THF, (3-hydroxytetrahydrofuran-2-yl)methyl phosphate.

*Corresponding author at: D.O.Z. (tel.: +7(383)3635128, fax: +7(383)3635153, e-mail: dzharkov@niboch.nsc.ru) or G.A.N. (tel.: +7(383)3635126, fax: +7(383)3635153, e-mail: nevinsky@niboch.nsc.ru)

Introduction

Genome of all living beings exists in a dynamic equilibrium between ongoing DNA damage and reversal of the damage, a process known as DNA repair ¹. Decrease in DNA repair capacity ultimately manifests itself in the form of mutagenesis, carcinogenesis, or cell death, and is implicated in a number of human diseases. DNA repair is crucial both for rapidly proliferating cells, in which lesions in DNA interfere with replication fork progress and may be converted into mutations upon replication, and for terminally differentiated cells, which sometimes have to maintain their genome integrity for the entire lifespan of the organism and have cell division-dependent checkpoints downregulated or turned off ². Several pathways have been defined in most organisms, including direct reversal, base excision repair (BER), nucleotide excision repair, mismatch repair, non-homologous end-joining, and recombination repair ¹. Of those, BER, which removes small non-bulky lesions, the most abundant type of spontaneous and induced DNA lesions, seems to be of the greatest importance in multicellular animals, judging from the embryonic lethality of knockouts inactivating the whole pathway ³. In the course of BER, one of several enzymes belonging to the class of DNA glycosylases excises a damaged base from DNA, leaving an apurinic/apyrimidinic (AP) site; then an AP endonuclease cleaves DNA at the AP site providing a free 3'-OH terminus, which is further used by a DNA polymerase to incorporate a normal dNMP. Finally, DNA ligase restores the integrity of the formerly damaged strand ¹.

A developing embryo displays more active cell proliferation than could be observed at any other stage of the organism's life cycle ⁴. Therefore, DNA repair is crucial during early embryonic development to support the fast cell division. Later, during organogenesis, DNA damage may lead to defects in cell division, migration, and interactions, producing congenital abnormalities ⁵. Recent studies also show that regulated and directed DNA damage together with its repair serves for fast reversion of epigenetic methylation, at least in vertebrates ⁶.

Mechanisms of the BER pathway and its interplay with other cellular processes have been extensively studied over the past decades⁷. However, this was mostly done in surprisingly few model objects, such as *E. coli*, yeast, mouse and human cells. While molecular aspects of embryonic development of mammals, including DNA damage and repair, are of great interest, such studies are complicated by the intrauterine mode of mammalian reproduction. Echinoderms, sea urchins in particular, are widely exploited in modern biology as easily accessible models of development in Deuterostomia, a superphylum where vertebrates belong, but this group is very poorly characterized with respect to BER. In sea urchins, only sporadic observations of individual activities in a few species, at a few developmental stages are available. For instance, the presence of uracil–DNA glycosylase activity was detected in early embryos of *Sphaerechinus granularis*⁸, and a functional Xth family AP endonuclease was cloned from *Paracentrotus lividus*⁹. Overall time courses of disappearance of DNA damage induced by various genotoxic assaults in adult sea urchin cells suggest that full BER is functional in several species^{8, 10, 11}.

We have investigated profiles of several BER activities in the embryonic development of *Strongylocentrotus intermedius*, a sea urchin species common in the Sea of Japan. A species from the same genus, *S. purpuratus*, which inhabits the West Coast of the United States, serves as a standard model of echinoderm development and has its genome sequenced, providing a useful basis for BER analysis in this class of animals. Our results suggest that dynamics of specific BER activities in sea urchin embryogenesis may reflect unique genotoxic challenges at various stages of development.

Results

Sea urchin genome encodes a complete set of base excision repair genes

Although the genome of *S. intermedius* has not been sequenced, a full genomic sequence is available for a closely related Eastern Pacific species, *S. purpuratus*^{12, 13}. We have searched the SpBase, the genomic database of *S. purpuratus*¹³, and additionally GenBank non-redundant database, using BLAST to identify sequences homologous to known BER proteins from human and *E. coli* (Table 1). The sea urchin genome contained genes encoding DNA glycosylases of uracil–DNA glycosylase structural superfamily (homologs of human UNG, TDG, and SMUG1) and Nth structural superfamily (homologs of human NTHL1, MUTYH, MBD4 and OGG1) but apparently lacked functional homologs of Fpg/Nei structural superfamily (*E. coli* Fpg and Nei, human NEIL1, NEIL2 and NEIL3, see Discussion). Unlike human cells that do not have homologs of *E. coli* Nfo AP endonuclease but contain APEX1 and APEX2 homologous to *E. coli* Xth protein, *S. purpuratus* possesses AP endonucleases belonging to both major structural

superfamilies of these proteins: exonuclease III-like and endonuclease IV-like. All human DNA polymerases and DNA ligases, as well as accessory proteins (FEN1, XRCC1, PARP1, PCNA, 9-1-1 factor subunits) participating in both short-patch and long-patch BER were found to have homologs in the sea urchin genome (Table 1). The homology between sea urchin and human sequences was considerable, with highly conserved catalytic domains and more divergent N- or C-terminal extensions (see Supplementary Fig. S1 for an example alignment of uracil-DNA glycosylase sequences). Overall, it can be concluded that *S. purpuratus* and, by inference, *S. intermedius* possesses a full set of BER enzymes required for removal of most lesions that are repaired through this pathway in other species.

Activities of BER enzymes in embryo extracts

In total, we have collected samples from 12 developmental stages representing the development from cleavage (two blastomers) to mid-pluteus. In the beginning of this period, the embryo resides inside the fertilized egg envelope and hatches at stage 12 (blastula), which then develops into a free-floating larva (the prism and later the pluteus). The embryos were lysed using a protocol that we had successfully applied earlier to the analysis of DNases from *S. intermedius* sperm and early embryos^{14, 15}. As the protein composition of the embryo changes during the development, the storage proteins, such as the 159-kDa major yolk protein (MYP), disappear at later stages^{16, 17}. Most BER proteins are small in size (< 60 kDa). Therefore, to provide a more meaningful estimate of BER enzymes activity, comparable between different stages, we calculated the specific activity of BER enzymes using an adjusted protein concentration, obtained after subtracting the fraction of protein staining in the large size zone (> ~90 kDa on a Laemmli system gel), dominated at early stages by MYP and other storage proteins, from the total Coomassie blue staining in a gel lane. Activities of several BER enzymes were then measured using oligonucleotide-based assays, which are easily interpreted and often employed in DNA repair studies in cell extracts of various nature. When possible, the cleavage was corrected for non-specific cleavage of an undamaged oligonucleotide with the same sequence except for the position of the lesion.

Uracil–DNA glycosylase activity

To follow the dynamics of uracil-DNA glycosylase activity, we have used a single-stranded 23-mer oligodeoxyribonucleotide substrate that contained a single deoxyuridine residue in the 10th position. Single-stranded DNA is a preferential substrate for human UNG and *E. coli* Ung enzymes¹⁸, and the high conservation of *S. purpuratus* XP_791566.1 protein suggests that the mode of interaction with DNA is the same in the sea urchin gene (Supplementary Fig. S1, Table

1). Non-specific nuclease degradation, most of which is due to the major *S. purpuratus* Ca^{2+} , Mg^{2+} -dependent DNase^{14, 19}, was inhibited by the addition of EDTA. Fig. 2A shows a representative gel of cleavage of dU-containing substrate, and the gel is quantified in Fig. 2B. The reaction rate was determined from the initial slope of time course plot, corrected for non-specific substrate degradation, and used to calculate the specific activity of *S. intermedius* uracil–DNA glycosylase at different development stages. The activity was suppressed by phage PBS2 Ugi protein, a specific inhibitor of uracil–DNA glycosylases related to *E. coli* Ung and human UNG enzymes (Fig. 2C).

As can be seen from Fig. 2D, the specific activity of uracil–DNA glycosylase was quite low until hatching of the late blastula (Stage 12) and then increased almost exponentially, reaching a maximum at 52 h post-fertilization (Stage 25). At the last sampled stage, the specific activity decreased but still remained much higher than early in the development.

8-Oxoguanine–DNA glycosylase activity

Since eukaryotic 8-oxoguanine–DNA glycosylase (OGG1) in all studied species is exclusively specific for double-stranded substrates containing an oxoG:C pair, a 23-mer duplex containing this pair was used as a substrate. However, when we have used the same reaction conditions as for uracil–DNA glycosylase, we could detect no appreciable substrate cleavage (data not shown). This is likely due to two reasons: if measured in parallel by the same type of assay, 8-oxoguanine–DNA glycosylase is usually less abundant than its uracil-specific counterpart in eukaryotes^{20, 21}, and OGG1 is a low-turnover enzyme, remaining tightly bound to the abasic product and displaced from it by APEX1 AP endonuclease²². Therefore, we eliminated EDTA from the reaction mixtures and carried the assays in the presence of 1 mM MgCl_2 to activate AP endonucleases in the lysates. Under these conditions, the oxoG:C substrate was cleaved (Fig. 3A). However, Mg^{2+} also activated non-specific DNases, most likely the Ca^{2+} , Mg^{2+} -dependent DNase abundant in the *S. intermedius* early development^{14, 19}. This was evident in the degradation of a control G:C duplex and required correction for the calculation of specific activity (Fig. 3B). Of note, cleavage of the oxoG:C substrate was also followed by partial 3'→5' degradation, making the product shorter than that resulting from oxoG:C duplex cleavage by *E. coli* 8-oxoguanine–DNA glycosylase, Fpg (compare the mobility of the product bands in Lanes 1 and 2–5, Fig. 3A). We have earlier observed similar 3'→5' degradation by human APEX1 in a reconstituted system of human oxoG repair²³. The specific activity of 8-oxoguanine–DNA glycosylase followed the profile generally opposite to that of uracil–DNA glycosylase: the activity was easily observed from the earliest stages of development but steadily

decreased after blastula hatching (Stage 12; Fig. 3C). However, the magnitude of the specific activity changes was much less than observed for uracil–DNA glycosylase.

In addition, we have profiled the embryo lysates using the duplex oligonucleotide substrates containing the mispairs 5,6-dihydrouracil:G (substrate for eukaryotic NTHL1 and NEIL1^{24,25}), 8-oxoadenine:C (substrate for OGG1 and NEIL1²⁶), hypoxanthine:T (substrate for MPG²⁷), or A:oxoG (substrate for MUTYH²⁸). However, we have been unable to detect any cleavage over the background with these duplexes, suggesting that the *S. intermedius* enzymes with these substrate specificities, if present in the developing embryo, are of low abundance.

AP endonuclease activity

The substrate for AP endonuclease assay was an oligonucleotide duplex containing a single residue of (3-hydroxytetrahydrofuran-2-yl)methyl phosphate (THF), an AP site analog that does not contain a hemiacetal moiety at C1' and thus is not cleaved by AP lyases such as OGG1. Since the Xth family AP endonucleases are Mg²⁺-dependent, the reactions were carried out in the presence of 1 mM MgCl₂, and non-specific degradation of an undamaged G:C-containing duplex was used to correct for the background cleavage. Fig. 4A shows that the AP endonuclease activity generally increased over time during the embryo development, although the latest stage experienced a drop in the activity.

Gap-filling DNA polymerase activity

BER can proceed through two sub-pathways, short- and long-patch, with the former dominating in the eukaryotes²⁹. Short-patch BER, which replaces a single damaged nucleotide in DNA, wholly depends on DNA polymerase β (POLβ) whereas long-patch BER is initiated by POLβ and continued by DNA polymerases δ or ε. Reflecting the place of POLβ in the sequence of BER mechanistic events, the preferable substrate for this DNA polymerase is DNA with a one-nucleotide gap³⁰. We used such a substrate (Fig. 1A) and dATP to evaluate the polymerase gap-filling activity that may be relevant for BER.

As shown in Fig. 4B, the gap-filling polymerase specific activity was quite high at the earliest stages of development, when the embryo undergoes fast cleavage, and sharply decreased at the blastula stages. Then, a burst of activity was observed at Stage 12, when blastulae hatch, followed by uniformly low specific activity afterwards. It should be noted that due to the presence of DNA polymerase cofactor Mg²⁺ in the reaction mixture and the concomitant non-specific substrate degradation, the actual gap-filling activity may be partially masked, yet the differences between the stages were quite clearly observed.

Discussion

Dynamics of DNA repair activities in the development of multicellular organisms is currently under active scrutiny with respect to a narrow set of BER enzymes specializing in the erasure of epigenetic marks from DNA⁶. However, information on the genome defense function of BER in development is quite fragmentary. Protection of the genome at embryogenesis is extremely important for two reasons. First, cells of the developing animal embryo divide much more rapidly than in the adults and failure to repair their DNA may lead to mutations, cell cycle disturbance or unregulated cell death manifesting in teratogenesis⁵. Second, various kinds of DNA damage were shown to disrupt binding of transcription factors involved in developmental regulation of a number of genes, including AP-1, Sp1, NF- κ B, CREB, etc.^{31,32}

Several studies followed DNA damage and repair in the developing zebrafish (*Danio rerio*), the most informative model in the developmental genetics of vertebrates³³. 8-oxoguanine–DNA glycosylase *ogg1* mRNA is enriched in the midbrain and heart tube of zebrafish embryos. *Ogg1* seems to be required for correct axonal growth and gross brain morphology; morpholino knockdown of *ogg1* significantly increases the level of oxoG and phosphorylated γ H2AX histone, a strand break marker, and changes the expression of an array of cell cycle checkpoint, apoptosis, and neurogenesis genes in the brain³⁴. In the cardiovascular system, *ogg1* knockdown disrupts cardiomyocyte production and leads to small heart, heart oedema, and a drop in the heart rate³⁵. A similar spectrum of cardiovascular abnormalities plus erythropoiesis deficiency, eye and notochord malformation results from a knockdown of AP endonuclease, the next enzyme in the BER pathway³⁶. Uracil–DNA glycosylase (*Unga*) mRNA is maternally supplied, and the level of protein increases ~4-fold from the zygote to the sphere (mid-blastula) stage; however, *Unga* in early zebrafish embryos seems to be involved to active epigenetic demethylation rather than genotoxic stress alleviation³⁷.

Observations of genome-defense DNA repair in other vertebrates are less systematic and mostly limited to rodents. In mouse embryos, the total level of *ung* mRNA rises dramatically between 7 and 11 days post coitum (dpc) and then gradually decreases³⁸; in rats, the same increase takes part between days 11 and 12 of gestation³⁹. However, at least in rats, this mRNA increase is at variance with the protein level or activity, which actually falls at this time³⁹; in several rat organs, uracil–DNA glycosylase activity peaks on or around birth and then sharply decreases⁴⁰. Another DNA glycosylase following a sharp increase pattern was *Nei1*, whose mRNA peaked at day 17 in mice⁴¹. An increase was also observed for murine *ogg1* from day 6.5 but it was more gradual⁴¹. In contrast, *mpg* mRNA level gradually decreases in mice from 7.5 dpc onward⁴². A decrease from day 14 of gestation was also observed in the rat brain for the

major isoform of MutY homolog; notably, this was accompanied with an appearance of other isoforms of the enzyme⁴³.

Drosophila and *Caenorhabditis elegans*, two leading invertebrate models of development, belong to Protostomia and so are less relevant to vertebrate embryogenesis than sea urchins. Notably, genomes of many protostomes seem to lack the full complement of vertebrate BER genes, suggesting alternative ways of repairing unavoidable endogenous lesions. For example, *Drosophila* has no uracil–DNA glycosylase homologs, yet two poorly characterized activities removing uracil from DNA either as a free base or as part of short oligonucleotides have been described from larvae of various ages^{44, 45}. Larval tissues of *Drosophila* contain a greatly elevated level of uracil, whereas imaginal discs seem to support active uracil removal and prevention of dUMP incorporation⁴⁶. Expression of *oggl* in the larvae also seems to be limited to imaginal discs⁴⁷. Uracil–DNA glycosylase is found in *C. elegans* embryos but its knockout has no consequences for the embryonic development⁴⁸.

We have selected *S. intermedius* for this study based both on the local availability in the Northwest Pacific and an assumption that this species shares the developmental features and sequence homology with the model congeneric species *S. purpuratus*, which inhabits the west coast of North America. The *S. purpuratus* genome encodes homologs of all proteins participating in BER in humans except having two DNA glycosylases of Fpg/Nei family instead of three in humans. Additionally, a homolog of bacterial endonuclease IV (Nfo) is present in *S. purpuratus* but not in humans.

A recent quantitative transcriptome study^{49, 50} established 72-h developmental profiles of expression for ~21,000 *S. purpuratus* genes (database available at <http://www.spbase.org:3838/quantdev/>). Direct comparison of these mRNA data with our enzyme activity data is complicated by discordance of the sampled time points; for instance, the first 18 h of development, including the hatching, are covered by 7 points in our study but only 2 points in^{49, 50}. Nevertheless, a side-by-side comparison reveals surprisingly little parallels between mRNA levels and enzyme activity. Uracil–DNA glycosylase activity, which increased by more than an order of magnitude after gastrulation, was actually accompanied with a decrease of a similar scale in the *udg* mRNA abundance, and mRNA levels remained relatively constant after 24 h of development. For *oggl*, the mRNA increased sharply during 0–18 h and then also remained relatively constant. AP endonucleases showed two distinct patterns of expression: *ape* mRNA steadily rose to a maximum at 30 h and then fell back to the early-embryo levels, yet the overall magnitude of change was only ~3-fold. mRNAs for the second Xth-like AP endonuclease, *apex2*, and for the Nfo-like AP endonuclease, *en_IV*, showed a time course very similar to that of *udg*, with a peak very early in development followed by a sharp drop. In fact,

udg, *apex2*, and *en_IV* were classified into one expression cluster⁵⁰. A similar behavior was also seen for *polb* but with a somewhat lower peak at 10 h. Although we did not measure DNA ligase activity, it is noteworthy that DNA ligase III, *dnl3*, was expressed in the same cluster with *oggl*, in view of the interactions between these two proteins in short-patch BER²⁹. Overall, however, changes in the expression of the BER pathway did not occur in concordance, and did not correlate with the enzyme activities that we have assayed, which may be due to regulation of the abundance of BER participants at the level of protein activity or stability rather than mRNA or protein synthesis. Our attempts to follow levels of *S. intermedius* BER proteins by Western blotting using antibodies raised to their human homologs were unsuccessful, likely due to poor cross-reactivity between these particular human and echinodermal antigens.

Since the same lesion can usually be processed by functionally redundant BER enzymes, the identity of activities we assayed in the extracts may be supported only indirectly. Single-stranded DNA containing uracil can be digested by uracil–DNA glycosylase Udg and single-strand-selective monofunctional uracil–DNA glycosylase Smug1⁵¹. Since UNG comprises ~90% of the uracil-removing activity in mammalian cells, and since uracil excision in our experiments was sensitive to Ugi protein (Fig. 2D), a specific inhibitor of UNG-like but not SMUG1-like enzymes, Udg is the primary candidate for the assayed activity. 8-Oxoguanine is most likely excised by Ogg1, the major eukaryotic glycosylase for this lesion⁵². Of three AP endonuclease homologs found in the *Strongylocentrotus* genome, En_IV probably does not contribute to the activity measured in our work, since enzymes of the Nfo family are Mg²⁺-independent and no activity was observed in the absence of Mg²⁺. Based on the relative abundance of APEX1 and APEX2, in mammalian cells, Ape seems a better candidate for the major *S. intermedius* AP endonuclease. Finally, of eukaryotic DNA polymerases, POLβ prefers DNA containing small gaps as a substrate³⁰ and is also the most abundant⁵³ so our assay likely reflects the activity of DNA polymerase β in the sea urchin cells. It should also be reiterated that the lack of some activities tested for (such as NTHL1-, NEIL1-, MPG-, and MUTYH-like) does not necessarily imply their absence but may be due to low level, expression in a limited number of specific cells, masking by other activities (e. g., nucleases), or suboptimal reaction conditions.

Abrupt changes in the environmental conditions expose the developing embryo to specific physiological assaults, including genotoxic ones. In humans and other viviparous animals, oxidative stress at birth is amply documented⁵⁴. Aquatic organisms experience similar kind of stress after hatching, when a protective egg envelope is discarded. In our profiles, embryo hatching was associated with a sustainable increase in the activity of uracil–DNA glycosylase and a temporary peak in the activity of gap-filling DNA polymerase. In embryos of another saltwater invertebrate, the brine shrimp *Artemia salina*, uracil–DNA glycosylase activity

increases during pre-emergence from the resting cyst⁵⁵. A number of DNA-damaging chemicals have been found in seawater, halogen oxides, reactive nitrogen species, and methyl halides being among the most abundant natural genotoxicants^{56, 57}. It is possible that a transition to the open marine environment requires adjustment of the embryo's DNA repair capacity for certain lesions, e.g., products of base deamination that are easily induced by reactive nitrogen species⁵⁸. In addition, development-specific genotoxic effects can be generated endogenously. For example, MYP, the major storage protein in *Strongylocentrotus* eggs, is a transferrin-like protein containing a Fe³⁺ binding site¹⁶. When cleaved in the course of early embryonic development¹⁷, MYP can release iron, which would then catalyze Fenton-like reactions and produce reactive oxygen species. This could explain a need for maintenance of high Ogg1 activity early in development.

Overall, our study underscores the temporal heterogeneity of DNA repair processes in animal development. Technical advances in quantitative nucleic acid-based assays, such as microarrays and real-time PCR, made them currently preferred instruments for studying the dynamics of biological systems. However, mRNA levels often do not parallel the extent of biochemical or other function, and have to be supplemented with proteomics, metabolomics, and wisely chosen enzyme assays. The sea urchin model, due to the easiness of genetic and biochemical manipulation, may prove useful for understanding the interplay between DNA damage, DNA repair, and development using a combination of omics and functional approaches.

Experimental

Oligonucleotides and enzymes

E. coli uracil-DNA glycosylase and phage PBS2 Ugi protein were purchased from New England Biolabs (Ipswich, MA). *E. coli* Fpg and human APEX1 were overproduced and purified as described^{22, 59}. Human DNA polymerase β was a kind gift of Dr. Svetlana N. Khodyreva (Institute of Chemical Biology and Fundamental Medicine). Structures of the DNA lesions and sequences of the oligonucleotides used to construct DNA substrates are given in Fig. 1. The oligonucleotides were end-labeled using γ [³²P]-ATP (Laboratory of Biotechnology, Institute of Chemical Biology and Fundamental Medicine) and T4 polynucleotide kinase (Biosan, Russia) according to the manufacturer's instructions, purified by reverse-phase chromatography on a Nensorb C₁₈ resin (PerkinElmer, Waltham, MA), and, if needed, annealed to a 2-fold molar excess of an unlabeled complementary strand and downstream primer.

Sea urchin embryo growth and extract preparation

All spawning and development procedures were carried out at 20°C in sea water sterilized by filtration through a 0.45 µm filter (Agilent Technologies, Santa Clara, CA). Adult specimens of *S. intermedius* were collected at the PIBOC Marine Experimental Station (Troitsa Bay area of the Peter the Great Bay, Sea of Japan) during the natural spawning season (August–September). Gamete release was induced by intracoelomic injection of 0.5 M KCl, and oocytes and sperm were isolated as described^{60, 61}. The unfertilized eggs in 100 ml of sea water were mixed with the concentrated suspension of sperm (2–5 ml) and after 2 min the mixture was diluted to 1 l. The eggs were allowed to settle down by gravity and washed with sea water 2–3 times to remove excess sperm. The fertilization efficiency was estimated by assessing the fertilization envelope elevation under a phase contrast microscope; the samples containing > 90–95% fertilized eggs were used. The embryos were grown in open 10-l vessels with mechanical mixing (50 rpm); the initial density of embryos was 3000 per ml. After blastula hatching, the embryo suspension was diluted twofold and counted; the density of embryos was 1200–1500 per ml. At the required times, 400–1500 ml aliquots were centrifuged at 4°C at 2000×g until a pellet formed and supernatant clarified, and the pellets were frozen at –70°C until analysis.

To prepare extracts, the cells were thawed on ice and resuspended in five volumes of ice-cold lysis buffer containing 10 mM Tris–HCl (pH 8.0), 1 M NaCl, 1 mM dithiothreitol (DTT), 1 mM ethylenediaminetetraacetate (EDTA), 0.5% Triton X-100, and 0.3 mM phenylmethylsulfonyl fluoride. Lysis was effected by sequential passage through syringe needles of decreased inner diameter (gauge 18, 19, 20, and 22), twice through each needle, followed by homogenization in a Dounce glass tissue grinder. The homogenates were centrifuged for 20 min at 4°C at 14,000×g and dialyzed in 1.5-kDa cutoff bags against two 1-l changes of 10 mM Tris–HCl (pH 8.0). The dialysates were supplemented with DTT to 1 mM and glycerol to 9%, aliquoted, and stored at –70°C. Total protein concentrations in the extracts were determined by Bradford staining with bovine serum albumin as a standard. Concentrations of medium- and low-molecular-weight proteins was determined after resolving the extracts by 12% SDS-polyacrylamide gel electrophoresis (Laemmli system) and staining with Coomassie Blue R250 with different amounts of bovine serum albumin run on the same gel as a standard; the concentrations measured in this way were used to calculate specific enzyme activities (see Results).

Enzyme activity assays

For analysis of uracil–DNA glycosylase activity, the substrate was a single-stranded 23-mer oligonucleotide containing a single deoxyuridine residue. For analysis of other DNA glycosylase activities, the substrates were 23-mer oligonucleotide duplexes containing pairs oxoG:C, 8-oxoadenine:C, dihydrouracil:G, hypoxanthine:T, or A:oxoG (Fig. 1). The thawed extracts (50 µl)

were supplemented with either EDTA (5 mM) or MgCl₂ (1 mM) and the substrate (50 nM), and incubated at 37°C. If necessary, the extracts were diluted in the storage buffer (see above) before adding EDTA and the substrate to achieve time course linearity. In parallel control reactions, undamaged oligonucleotides identical to the substrates except at the site of the damage (C for uracil–DNA glycosylase, G:C for 8-oxoguanine–DNA glycosylase) were added. Aliquots (5 µl) were withdrawn at 2–120 min, and the reaction was stopped by adding 5 µl of 0.2 M NaOH to the final and heating for 2 min at 95°C. The solution was neutralized by 5 µl of 0.2 M HCl and mixed with 8 µl of gel loading dye (80% formamide, 20 mM Na-EDTA, 0.1% xylene cyanol, 0.1% bromophenol blue).

For analysis of AP endonuclease activity, the substrate was a 23-mer oligonucleotide duplex containing a (3-hydroxytetrahydrofuran-2-yl)methyl phosphate (THF), an AP site analog resistant to alkali, heating and bifunctional glycosylases, opposite C. The thawed extracts (50 µl) were supplemented with MgCl₂ (1 mM) and the substrate (50 nM), and incubated at 37°C. In control, undamaged G:C oligonucleotide was used. Aliquots (5 µl) were withdrawn at 2–20 min, and the reaction was stopped by adding 5 µl of the gel loading dye and heating for 2 min at 95°C.

For analysis of DNA polymerase activity, the substrate was constructed by annealing a 23-mer template, a 5'-³²P-labeled 10-mer primer, and a 12-mer downstream primer to contain a single-nucleotide gap (Fig. 1A). The thawed extracts (18 µl) were mixed with the 10× buffer stock to the final concentrations: 10 mM Tris–HCl (pH 8.0), 25 mM KCl, 10 mM MgCl₂, 1 mM DTT, 100 µM dATP, and 100 nM substrate. The reaction was incubated at 20°C for 5 min and terminated by adding 10 µl of the gel loading dye and heating for 2 min at 95°C.

In all cases, the reaction products were resolved by denaturing 20% polyacrylamide gel electrophoresis. The gels were imaged using Molecular Imager FX system (Bio-Rad Laboratories, Hercules, CA) and quantified with Quantity One v4.6.3 software (Bio-Rad). Initial rates were determined from the slope of the linear part of the reaction progress curve, corrected for non-specific degradation of the control substrate. All reported values are mean ± s.d. of three independent experiments.

Acknowledgements

This research was supported by the Presidium of the Russian Academy of Sciences (MKB 6.12), by Russian Foundation for Basic Research (13-04-00211 and 14-04-01879), and funds from the Siberian Division of the Russian Academy of Sciences. We thank Dr. Svetlana N. Khodyreva

(Institute of Chemical Biology and Fundamental Medicine) for a gift of DNA polymerase β , and Dr. Olga I. Sinitsina (Institute of Cytology and Genetics, Novosibirsk) for valuable discussion.

References

1. E. C. Friedberg, G. C. Walker, W. Siede, R. D. Wood, R. A. Schultz and T. Ellenberger, *DNA Repair and Mutagenesis*, ASM Press, Washington, D.C., 2006.
2. T. Nospikel, *Neuroscience*, 2007, **145**, 1213-1221.
3. E. C. Friedberg and L. B. Meira, *DNA Repair*, 2006, **5**, 189-209.
4. M. A. Ciemerych and P. Sicinski, *Oncogene*, 2005, **24**, 2877-2898.
5. P. G. Wells, G. P. McCallum, K. C. H. Lam, J. T. Henderson and S. L. Ondovcik, *Birth Defects Res. C Embryo Today*, 2010, **90**, 103-109.
6. H. J. Lee, T. A. Hore and W. Reik, *Cell Stem Cell*, 2014, **14**, 710-719.
7. T. Iyama and D. M. Wilson, III, *DNA Repair*, 2013, **12**, 620-636.
8. R. Le Bouffant, P. Cormier, A. Cueff, R. Bellé and O. Mulner-Lorillon, *Cell. Mol. Life Sci.*, 2007, **64**, 1723-1734.
9. A. V. Cioffi, D. Ferrara, M. V. Cubellis, F. Aniello, M. Corrado, F. Liguori, A. Amoroso, L. Fucci and M. Branno, *Biochem. J.*, 2002, **365**, 833-840.
10. J. Loram, R. Raudonis, J. Chapman, M. Lortie and A. Bodnar, *Aquat. Toxicol.*, 2012, **124-125**, 133-138.
11. A. H. El-Bibany, A. G. Bodnar and H. C. Reinardy, *PLoS ONE*, 2014, **9**, e107815.
12. Sea Urchin Genome Sequencing Consortium, *Science*, 2006, **314**, 941-952.
13. R. A. Cameron, M. Samanta, A. Yuan, D. He and E. Davidson, *Nucleic Acids Res.*, 2009, **37**, D750-D754.
14. N. I. Menzorova and V. A. Rasskazov, *Biochemistry (Mosc.)*, 1980, **45**, 413-420.
15. V. V. Shastina, N. I. Menzorova, Y. T. Sibirtsev and V. A. Rasskazov, *Biochemistry (Mosc.)*, 2003, **68**, 582-592.
16. J. M. Brooks and G. M. Wessel, *Dev. Biol.*, 2002, **245**, 1-12.
17. Y. Yokota, T. Unuma, A. Moriyama and K. Yamano, *Comp. Biochem. Physiol. B Biochem. Mol. Biol.*, 2003, **135**, 71-81.
18. D. O. Zharkov, G. V. Mechetin and G. A. Nevinsky, *Mutat. Res.*, 2010, **685**, 11-20.
19. Y. T. Sibirtsev, N. I. Menzorova, V. V. Shastina and V. A. Rasskazov, *Dokl. Biochem. Biophys.*, 2001, **376**, 4-6.
20. S. Z. Imam, B. Karahalil, B. A. Hogue, N. C. Souza-Pinto and V. A. Bohr, *Neurobiol. Aging*, 2006, **27**, 1129-1136.

21. B. Karahalil, V. A. Bohr and N. C. de Souza-Pinto, *Anticancer Res.*, 2010, **30**, 4963-4971.
22. V. S. Sidorenko, G. A. Nevinsky and D. O. Zharkov, *DNA Repair*, 2007, **6**, 317-328.
23. R. D. Kasymov, I. R. Grin, A. V. Endutkin, S. L. Smirnov, A. A. Ishchenko, M. K. Saparbaev and D. O. Zharkov, *FEBS Lett.*, 2013, **587**, 3129-3134.
24. R. Venkhataraman, C. D. Donald, R. Roy, H. J. You, P. W. Doetsch and Y. W. Kow, *Nucleic Acids Res.*, 2001, **29**, 407-414.
25. M. M. Ali, T. K. Hazra, D. Hong and Y. W. Kow, *DNA Repair*, 2005, **4**, 679-686.
26. I. R. Grin, G. L. Dianov and D. O. Zharkov, *FEBS Lett.*, 2010, **584**, 1553-1557.
27. S. Adhikari, A. Üren and R. Roy, *J. Biol. Chem.*, 2007, **282**, 30078-30084.
28. M. Takao, Q.-M. Zhang, S. Yonei and A. Yasui, *Nucleic Acids Res.*, 1999, **27**, 3638-3644.
29. P. Fortini and E. Dogliotti, *DNA Repair*, 2007, **6**, 398-409.
30. A. M. Chagovetz, J. B. Sweasy and B. D. Preston, *J. Biol. Chem.*, 1997, **272**, 27501-27504.
31. M. K. Hailer-Morrison, J. M. Kotler, B. D. Martin and K. D. Sugden, *Biochemistry*, 2003, **42**, 9761-9770.
32. S. P. G. Moore, K. J. Toomire and P. R. Strauss, *DNA Repair*, 2013, **12**, 1152-1158.
33. A. Amsterdam and N. Hopkins, *Trends Genet.*, 2006, **22**, 473-478.
34. A. Gu, G. Ji, L. Yan and Y. Zhou, *DNA Repair*, 2013, **12**, 1094-1104.
35. L. Yan, Y. Zhou, S. Yu, G. Ji, L. Wang, W. Liu and A. Gu, *Exp. Cell Res.*, 2013, **319**, 2954-2963.
36. Y. Wang, C. C. Shupenko, L. F. Melo and P. R. Strauss, *Mol. Cell. Biol.*, 2006, **26**, 9083-9093.
37. D. Wu, L. Chen, Q. Sun, X. Wu, S. Jia and A. Meng, *J. Biol. Chem.*, 2014, **289**, 15463-15473.
38. H. Nilsen, K. S. Steinsbekk, M. Otterlei, G. Slupphaug, P. A. Aas and H. E. Krokan, *Nucleic Acids Res.*, 2000, **28**, 2277-2285.
39. R. K. Vinson and B. F. Hales, *Biochem. Pharmacol.*, 2002, **64**, 711-721.
40. Y. Weng and M. A. Sirover, *Mutat. Res.*, 1993, **293**, 133-141.
41. G. A. Hildrestrand, D. B. Diep, D. Kunke, N. Bolstad, M. Bjørås, S. Krauss and L. Luna, *DNA Repair*, 2007, **6**, 723-732.
42. N.-K. Kim, S.-H. Lee, T.-J. Sohn, R. Roy, S. Mitra, H.-M. Chung, J.-J. Ko and K.-Y. Cha, *Anticancer Res.*, 2000, **20**, 3037-3043.

43. H.-M. Lee, Z. Hu, H. Ma, G. H. Greeley, Jr, C. Wang and E. W. Englander, *J. Neurochem.*, 2004, **88**, 394-400.
44. A. R. Morgan and J. Chlebek, *J. Biol. Chem.*, 1989, **264**, 9911-9914.
45. A. Békési, M. Pukáncsik, V. Muha, I. Zagyva, I. Leveles, É. Hunyadi-Gulyás, É. Klement, K. F. Medzihradzsky, Z. Kele, A. Erdei, F. Felföldi, E. Kónya and B. G. Vértessy, *Biochem. Biophys. Res. Commun.*, 2007, **355**, 643-648.
46. V. Muha, A. Horváth, A. Békési, M. Pukáncsik, B. Hodoscsek, G. Merényi, G. Róna, J. Batki, I. Kiss, F. J. P. Vilmos, M. Erdélyi and B. G. Vértessy, *PLoS Genet.*, 2012, **8**, e1002738.
47. C. Dherin, M. Dizdaroglu, H. Doerflinger, S. Boiteux and J. P. Radicella, *Nucleic Acids Res.*, 2000, **28**, 4583-4592.
48. N. Nakamura, H. Morinaga, M. Kikuchi, S.-I. Yonekura, N. Ishii, K. Yamamoto, S. Yonei and Q.-M. Zhang, *Mutagenesis*, 2008, **23**, 407-413.
49. Q. Tu, R. A. Cameron, K. C. Worley, R. A. Gibbs and E. H. Davidson, *Genome Res.*, 2012, **22**, 2079-2087.
50. Q. Tu, R. A. Cameron and E. H. Davidson, *Dev. Biol.*, 2014, **385**, 160-167.
51. T. Visnes, B. Doseth, H. S. Pettersen, L. Hagen, M. M. L. Sousa, M. Akbari, M. Otterlei, B. Kavli, G. Slupphaug and H. E. Krokan, *Philos. Trans. R. Soc. Lond. B Biol. Sci.*, 2009, **364**, 563-568.
52. S. S. David, V. L. O'Shea and S. Kundu, *Nature*, 2007, **447**, 941-950.
53. L. A. Loeb and R. J. Monnat, Jr., *Nat. Rev. Genet.*, 2008, **9**, 594-604.
54. O. D. Saugstad, Y. Sejersted, R. Solberg, E. J. Wollen and M. Bjørås, *Neonatology*, 2012, **101**, 315-325.
55. D. J. Birch and A. G. McLennan, *Biochem. Soc. Trans.*, 1980, **8**, 730-731.
56. A. D. Anbar, Y. L. Yung and F. P. Chavez, *Global Biogeochem. Cycles*, 1996, **10**, 175-190.
57. M. J. Kim, D. K. Farmer and T. H. Bertram, *Proc. Natl Acad. Sci. U.S.A.*, 2014, **111**, 3943-3948.
58. B. Halliwell, *Mutat. Res.*, 1999, **443**, 37-52.
59. R. Gilboa, D. O. Zharkov, G. Golan, A. S. Fernandes, S. E. Gerchman, E. Matz, J. H. Kycia, A. P. Grollman and G. Shoham, *J. Biol. Chem.*, 2002, **277**, 19811-19816.
60. G. M. Wessel and V. D. Vacquier, *Methods Cell Biol.*, 2004, **74**, 491-522.
61. V. D. Vacquier and N. Hirohashi, *Methods Cell Biol.*, 2004, **74**, 523-544.
62. A. Marchler-Bauer, M. K. Derbyshire, N. R. Gonzales, S. Lu, F. Chitsaz, L. Y. Geer, R. C. Geer, J. He, M. Gwadz, D. I. Hurwitz, C. J. Lanczycki, F. Lu, G. H. Marchler, J. S.

- Song, N. Thanki, Z. Wang, R. A. Yamashita, D. Zhang, C. Zheng and S. H. Bryant, *Nucleic Acids Res.*, 2015, **43**, D222-D226.
63. G. A. Buznikov and V. I. Podmarev, in *Objects of Developmental Biology*, ed. B. L. Astaurov, Nauka, Moscow, 1975, pp. 188-216.
64. S. S. Parikh, C. D. Mol, G. Slupphaug, S. Bharati, H. E. Krokan and J. A. Tainer, *EMBO J.*, 1998, **17**, 5214-5226.
65. F. Sievers, A. Wilm, D. Dineen, T. J. Gibson, K. Karplus, W. Li, R. Lopez, H. McWilliam, M. Remmert, J. Söding, J. D. Thompson and D. G. Higgins, *Mol. Syst. Biol.*, 2011, **7**, 539.

Table 1 Homologs of the major BER proteins in the sea urchin genome

Role in BER	Structural superfamily	<i>E. coli</i>	<i>H. sapiens</i>	<i>S. purpuratus</i> *	% identity (overall/core) [‡]
DNA glycosylases	UDG-like	Ung	UNG	Udg; XP_791566.1	59/74
		Mug	TDG	Tdg; XP_791344.3, XP_011671297.1	25/68
		–	SMUG1	Smug1; XP_003723427.1	28/51
		–	MBD4	Mbd4; XP_783908.2	33/64
	Endonuclease III	Nth	NTHL1	Nth1; XP_793669.4	56/66
		–	OGG1	Ogg1; XP_791749.3, XP_011664878.1, XP_011664886.1	41/45
		MutY	MUTYH	Mutyh; XP_791369.3	42/51
	Fpg/Nei	Nei	NEIL1	Neil1; XP_011660809.1, XP_011670712.1	19/32
			NEIL2	Neh2; XP_011678332.1, XP_011682324.1	20/37
			NEIL3		(both to NEIL2)
Formyltransferase-like	–	MPG	Mpg; XP_786488.2	39/49	
	Exonuclease III	Xth	APEX1	Ape; XP_789515.3, XP_011677768.1	50/56
			APEX2	Apex2; XP_784420.3, XP_011665582.1	35/47
AP endonucleases	Endonuclease IV	Nfo	–	En_IV; XP_011667848.1	24/56
DNA polymerases	Family X	–	POLβ	Polb; XP_787665.3, XP_003729524.1	64/65
	Family B	PolB	POLδ	Pold [†] ; XP_011677355.1	69/70
POLε			Pole [†] ; XP_011673950.1	63/69	
DNA ligases	ATP-dependent	–	LIG1	Dnl1; XP_001180844.2	49/65
Scaffold protein		–	LIG3	Dnl3; XP_011671479.1	51/63
Nick sensor	–	–	XRCC1	Xrcc1; XP_011671396.1	38/46
Processivity factor	–	–	PARP1	Parp1; XP_001177436.3	47/53
Flap endonuclease	–	–	PCNA	Pcna; XP_011661657.1	30/31
Polymerase exchange factor	–	–	FEN1	Fen1; XP_001197560.2	59/62
			RAD9	Rad9; XP_011679156.1	29/44
			HUS1	Hus1; XP_786829.1	47/48
–	–	–	RAD1	Rad1; XP_794375.2	66/68

*Gene names and protein RefSeq record numbers (genome assembly v4.2)^{13,49}. When several records are indicated, they refer to different predicted protein isoforms.

[†]Catalytic subunit.

[‡]% identity between *S. purpuratus* and human protein sequences. For En_IV, % identity between *S. purpuratus* and *E. coli* Nfo is shown, since humans lack Nfo homologs. “Core” is the functional core of the protein composed of one or several conserved domains defined in the Conserved Domains Database⁶².

Table 2 Developmental stages analyzed in this study

Embryo collection time, h:min post fertilization	Stage number*	Stage*	Adjusted protein concentration, mg/ml
1:07	3	cleavage (2 blastomers)	4.1
2:20	5	cleavage (8 blastomers)	4.5
3:40	7	cleavage (32 blastomers)	4.4
7:15	10	mid-blastula 1	4.8
9:30	11	mid-blastula 2	4.3
11:00	12	late blastula 1 (hatched)	4.7
17:00	15	early gastrula 2	3.4
20:30	18	late gastrula 1	4.1
25:00	20	prism 1	3.0
39:30	24	early pluteus 3	1.3
52:00	25	mid-pluteus 1	1.0
60:00	26	mid-pluteus 2	2.0

*Stage assignment for *S. intermedius* development at 20°C, based on the time post fertilization⁶³.

Legends to figures

Fig. 1. DNA substrates used in this study. Panel A, sequences of oligonucleotides used to construct the substrates for DNA glycosylase and AP endonuclease activities (left) and DNA polymerase activities (right). For DNA glycosylase activities, X was 8-oxoguanine (oxoG), uracil (U), dihydrouracil, 8-oxoadenine, hypoxanthine, A, G, or C, and Y was C, G, T, or oxoG. For the AP endonuclease activity, X was THF, and Y was C. Panel B, structures of the DNA lesions studied. dR, deoxyribose moiety.

Fig. 2. **A**, image of a representative gel after 20% denaturing PAGE separating products of cleavage of ^{32}P -labeled oligonucleotide containing a dU residue (*lanes 1–7: lane 1, 5 min, lane 2, 10 min, lane 3, 20 min, lane 4, 30 min, lane 5, 60 min, lane 6, 90 min, lane 7, 120 min*) or dC at the same position (*lanes 8–10: lane 8, 2 min, lane 9, 20 min, lane 10, 120 min*). The substrate was incubated with Stage 10 embryo lysate for the indicated time. S, substrate, P, cleavage product. **B**, plot of the time course of the reaction shown in Panel A. *Filled circles*, dU-containing substrate, *open circles*, dC-containing substrate. **C**, inhibition of the dU-removing activity by Ugi protein. *Lane 1*, dU-containing substrate with no enzyme or extract; *lane 2*, treated for 10 min with 0.5 U/ μl *E. coli* uracil–DNA glycosylase; *lane 3*, treated for 30 min with Stage 10 embryo lysate in the presence of 0.2 U/ μl Ugi; *lane 4*, treated for 30 min with Stage 10 embryo lysate in the absence of Ugi. **D**, specific activity of uracil–DNA glycosylase at different stages of *S. intermedius* development, shown on a log scale.

Fig. 3. **A**, image of a representative gel after 20% denaturing PAGE separating products of cleavage of ^{32}P -labeled oligonucleotide containing an oxoG:C pair (*lane 2, 2 min, lane 3, 5 min, lane 4, 10 min, lane 5, 20 min*). *Lanes 1 and 6*: cleavage size marker, the same substrate cleaved at oxoG by purified *E. coli* Fpg protein. *Lanes 7 and 8*: intact size marker, the same substrate incubated without extract for 0 min (*lane 8*) or 20 min (*lane 7*). The substrate was incubated with Stage 3 embryo lysate for the indicated time. S, substrate, P, cleavage products. **B**, plot of the time course of the reaction shown in Panel A. *Filled circles*, oxoG:C-containing substrate, *open circles*, G:C-containing substrate (mean and s. d. of three independent experiments). **C**, specific activity of 8-oxoguanine–DNA glycosylase at different stages of *S. intermedius* development.

Fig. 4. **A**, gel showing the cleavage of a THF:C-containing duplex and control G:C duplex by embryo lysates from different stages of development. The stages and substrates are indicated in the figure. Lane 9, cleavage size marker: THF:C duplex incubated with 1.5 μM purified human

APEX1 (E) for 5 min. Lanes 10 and 11, intact size markers: THF:C and G:C duplexes, respectively, incubated without extract for 20 min. S, substrate, P, cleavage product. **B**, specific activity of AP endonuclease at different stages of *S. intermedius* development. **C**, gel showing gap filling by embryo lysates from different stages of development indicated in the figure. *Lane 9*, intact size marker: the gapped substrate duplex incubated without extract for 5 min. *Lane 10*, extension size marker: the gapped substrate duplex incubated with 500 nM purified human DNA polymerase β for 5 min. Pr, primer, Pr+1, primer extended by one nucleotide. Products of nuclease degradation of the primer are visible below the primer band. **D**, specific gap-filling DNA polymerase activity at different stages of *S. intermedius* development.

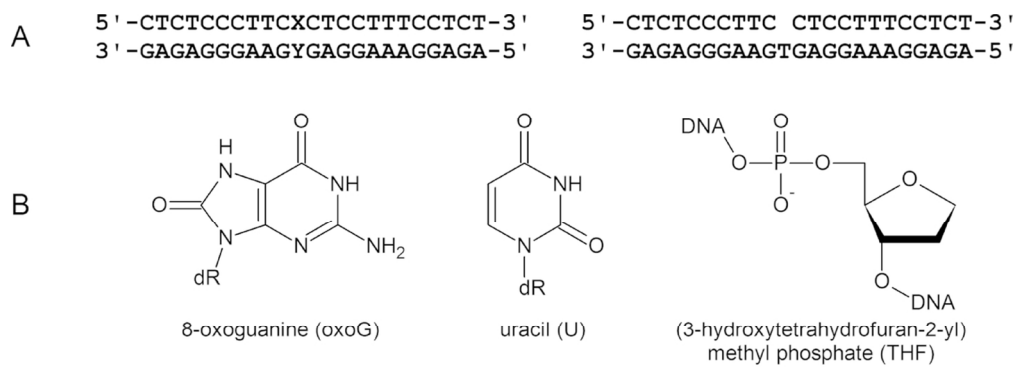


Figure 1 (two-column)

122x89mm (300 x 300 DPI)

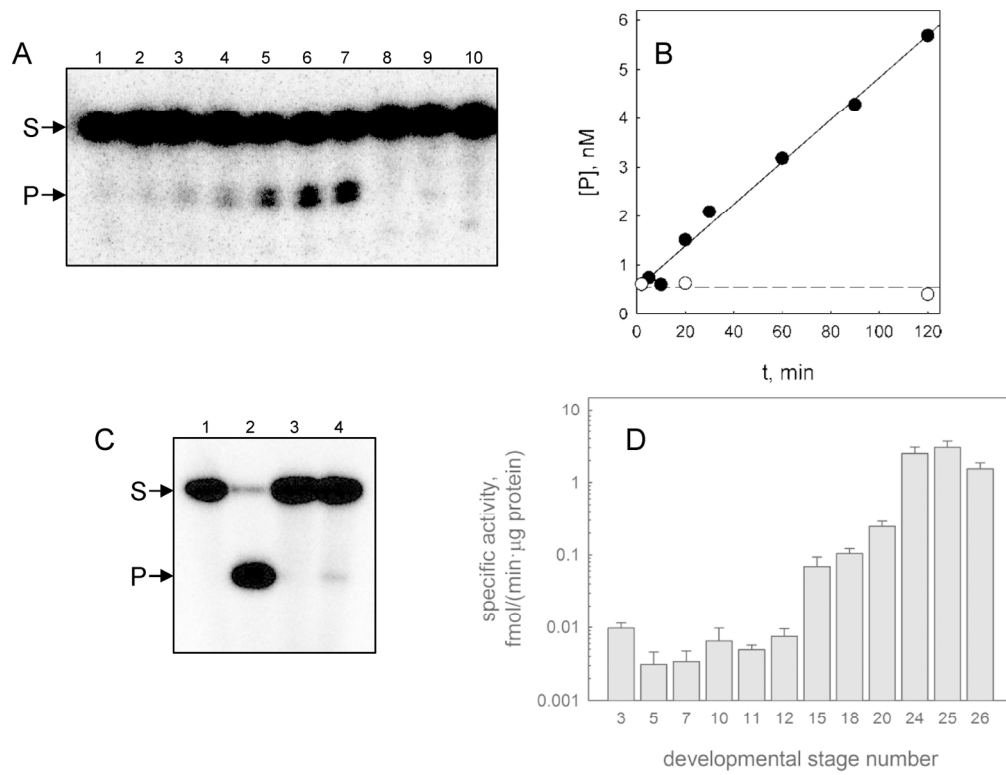


Figure 2 (two-column)

166x167mm (300 x 300 DPI)

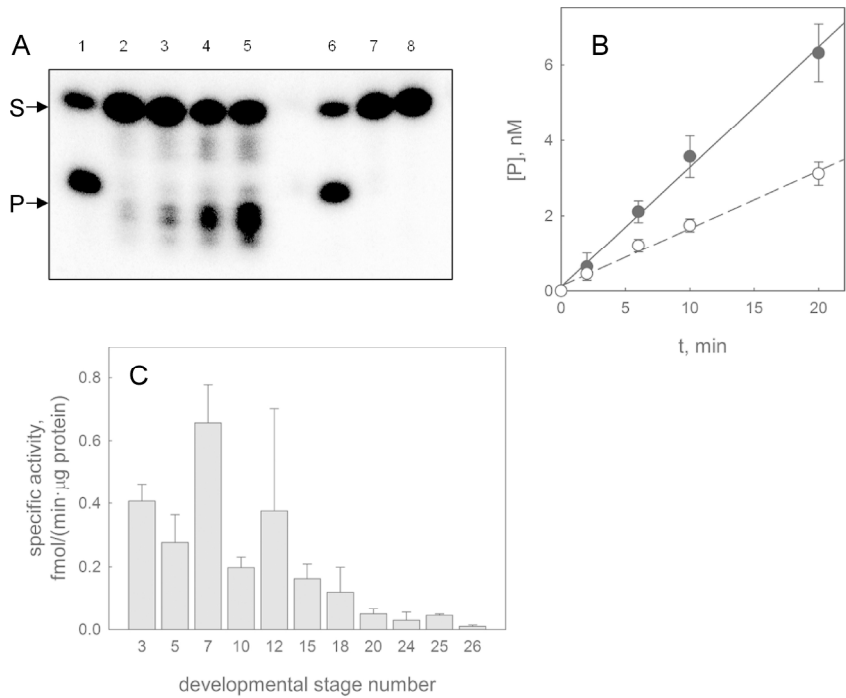


Figure 3 (two-column)

212x305mm (300 x 300 DPI)

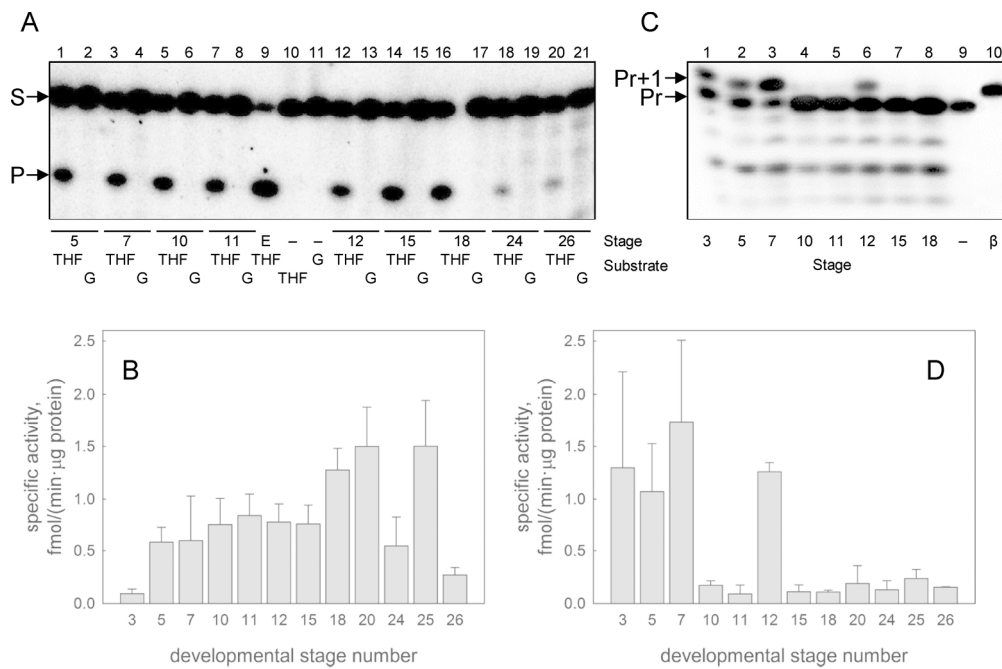


Figure 4 (two-column)

189x195mm (300 x 300 DPI)